Archives of Biochemistry and Biophysics 531 (2013) 100–109

Contents lists available at SciVerse ScienceDirect

Archives of Biochemistry and Biophysics

journal homepage: www.elsevier.com/locate/yabbi

Review

Differential scanning calorimetry as a tool for protein folding and stability

Christopher M. Johnson *

MRC Laboratory of Molecular Biology, Hills Road, Cambridge, CB2 0QH, United Kingdom

ARTICLE INFO

Article history:
Available online 27 September 2012

Keywords:
Differential scanning calorimetry
Protein stability
Protein folding
Equilibrium thermodynamics

ABSTRACT

Differential scanning calorimetry measures the heat capacity of states and the excess heat associated with transitions that can be induced by temperature change. The integral of the excess heat capacity is the enthalpy for this process. Despite this potentially intimidating sounding physical chemistry background, DSC has found almost universal application in studying biological macromolecules. In the case of proteins, DSC can be used to determine equilibrium thermodynamic stability and folding mechanism but can also be used in a more qualitative manner screening for thermal stability as an indicator for, ligand binding, pharmaceutical formulation or conditions conducive to crystal growth. DSC usually forms part of a wider biophysical characterisation of the biological system of interest and so the literature is diverse and difficult to categorise for the technique in isolation. This review therefore describes the potential uses of DSC in studying protein folding and stability, giving brief examples of applications from the recent literature. There have also been some interesting developments in the use of DSC to determine barrier heights for fast folding proteins and in studying complex protein mixtures such as human plasma that are considered in more detail.

1. Introduction

Measurements of the energetics of biological and biochemical processes using direct calorimetric methods was pioneered by a handful of academic groups in the 1960's and 1970's using instruments fabricated and assembled in the laboratory [1–5]. Early work was motivated by a desire to measure the fundamental thermodynamic driving forces behind the processes of protein stability, folding and binding interactions and focused mostly on proteins that were readily available in large quantities. Forty years on and the interpretation and prediction of the energetics of biological processes is still a somewhat elusive goal. The large and dominant role played by solvent, which is dynamic and difficult to visualise in high-resolution structures or quantify by other techniques, makes the contribution of interactions between molecules that can be visualised and manipulated (e.g., using mutation) difficult to understand. However, the legacy of these early efforts has lead to technological advances and commercial instrumentation that places calorimetry as a routine technique in most biophysics labs [6–8]. Current instrumentation uses only modest quantities of material and instrument operation is simple or even automated, making calorimetric methods a standard component of the biophysical characterization of even precious or difficult to obtain samples.

Differential scanning calorimetry (DSC)[1] was the earlier of the calorimetric methods developed for biological samples. It is now perhaps less popular compared with isothermal titration calorimetry (ITC) that measures interactions by mixing components at a fixed temperature. In contrast, DSC studies transitions, or processes that are induced by changes in temperature; most commonly increasing temperature leading to 'thermal melting'. Most biological molecules of interest undergo such phase transitions and so can be studied using DSC. The focus of this article is the application of DSC in studying protein folding and thermal stability ranging from its most basic applications in folding mechanism to applications in highly complex systems and heterogeneous samples. It uses a necessarily didactic style to highlight the full capabilities of the technique in studying the thermodynamics underlying biological processes. In many cases these possibilities are either forgotten or misused. Articles describing the use of DSC in studying intrinsically disordered proteins, nucleic acids or lipids can be found elsewhere [9–11].

2. Basic DSC measurement

In conventional up scanning mode DSC instruments monitor a small temperature difference between a reference cell that is filled with solvent and a sample cell that contains the protein of interest in an identical solvent. As the temperature of both cells is increased thermally induced processes occurring in the sample cell result in heat being absorbed (at least initially) and this produces a change

* Fax: +44 1223 213556.
E-mail address: cmj@mrc-lmb.cam.ac.uk

[1] Abbreviation used: DSC, differential scanning calorimetry; ITC, isothermal titration calorimetry.

0003-9861/$ - see front matter
http://dx.doi.org/10.1016/j.abb.2012.09.008

in the temperature difference relative to the reference cell. Heaters on the sample cell surface in a feedback circuit input additional electrical power to return the temperature difference to its initial value. This additional heat is proportional to the excess heat capacity of the thermally induced process. For simple proteins a single heat absorption peak is often observed in the scan, or 'thermogram', and, after correction for instrumental baseline, the transition baseline and normalisation to concentration, the peak can be integrated to give a direct calorimetric measurement of the enthalpy for the process (ΔH_{cal}) and a measure of the melting temperature (*Tm*).

$$\Delta H = \int_{T_0}^{T_1} Cp.dT \tag{1}$$

ΔH_{cal} can be compared with the indirectly determined van't Hoff enthalpy (ΔH_{vH}) that is obtained from the analysis of the thermogram. The van't Hoff analysis is based on the assumption of a transition between two states. It can be obtained without any concentration normalisation of the data since the '*per* mol' term is introduced from the gas constant, R. Comparison of ΔH_{cal} with the indirect model based ΔH_{vH} is, therefore, a method of verifying the assumed two-state model used in the van't Hoff analysis. It remains a common test of two state folding to check the equality of these enthalpies ($\Delta H_{vH}/\Delta H_{cal} = 1$) with values above 1 indicative of self association (e.g., as dimer, trimer etc.) and values below 1 indicative of unfolding via one or more intermediate states.

While such comparisons are valuable it is important to remember that the measured calorimetric enthalpy is determined by normalisation to protein concentration. Errors in the measurement of this concentration and the presence of low levels of already denatured protein or other minor impurities will all contribute to an inaccurate measure of ΔH_{cal}. Integration of the heat absorption peak also requires the use of a baseline that is 'intrinsic' to the protein being studied. This is normally produced by extrapolation of the pre- and post-transition baselines into the transition region and merging their slopes and levels in proportion to the 'progress' (extent) of the melting process. A number of alternative methods have also been discussed [12]. The baseline chosen is unlikely to have a significant effect on ΔH_{cal} for narrow, large enthalpy transitions, but smaller enthalpy systems or broad transitions originating from multiple overlapping transitions can be problematic.

A thermodynamic analysis of the DSC thermogram, yielding ΔH_{cal}, ΔH_{vH} and *Tm*, also pre-assumes equilibrium reversibility during the thermal denaturation process. Unfortunately, this is often not the case. The thermal denaturation of many proteins is accompanied by aggregation or irreversible denaturation at the high temperatures required for complete unfolding. To confirm equilibrium reversibility the observed thermogram should be 'repeatable' (i.e., once the DSC scan is complete the protein can be cooled, scanned again and demonstrate an essentially identical thermogram). The fitted ΔH_{cal}, ΔH_{vH} and *Tm* should also be independent of instrumental scan (heating) rate, indicating that the equilibrium is relaxing faster than the rate of temperature change, and, at least for simple monomeric proteins, be independent of protein concentration.

3. Measurement of absolute heat capacity

DSC data analysis can be performed on the simple apparent excess heat capacity following baseline subtraction and concentration normalisation. However, DSC can be used to determine the absolute heat capacity of the protein when account is taken of the heat capacity of the volume of solvent that is displaced from the sample cell by the protein. In the reference cell this is occupied by solvent. The calculation requires knowledge of the mass of protein used (m_{pr}), the partial specific volumes of protein and solvent ($\bar{v}_{pr}$ and $\bar{v}_{sol}$) as well as the heat capacity of the solvent used (Cp_{sol});

$$Cp_{pr} = Cp_{sol} \cdot \frac{\bar{v}_{pr}}{\bar{v}_{sol}} - \frac{Cp_{exp}}{m_{pr}} \tag{2}$$

Cp_{exp} is the measured excess heat capacity. Cp_{sol} can be determined using DSC by scanning the solvent against water which has a well established heat capacity over the experimental temperature range. A simpler and more reliable method avoids the additional processing by measuring the dependence of the apparent heat capacity of the protein on its concentration [13]. This method is applied direct to raw DSC data, without buffer baseline subtraction, (thereby avoiding the protein thermogram being the result of subtraction between two separate measurements) and has added statistical reliability from being derived by multiple measurements on the same protein. Measurements of absolute heat capacity require methodical technique and sample preparation. Degassing becomes very important. Similarly, exhaustive dialysis into the experimental solvent is required as relatively small mismatches in buffer can affect the data especially in the low temperature region of the thermogram.

The absolute heat capacity profile can be subject to the same fitting as the more simply processed thermogram. The absolute heat capacity is also a fundamental property of the native and denatured states of proteins and can give information about structure and flexibility in these states. Much of the early work on simple globular systems has shown that the absolute heat capacity of native and denatured proteins, and variation as a function of temperature, have common 'universal' values when normalised *per* gram protein [14]. Thus, it is easy to determine if a new system being studied has typical values for a globular protein or whether it has, for example, regions of disorder in its native state, which should increase its heat capacity, or a highly structured denatured state, which would lower the heat capacity at higher temperature.

4. DSC and equilibrium folding mechanisms

DSC data used in an analytical thermodynamic mode can obviously be very informative when the equilibrium folding mechanism is of interest. For example, variants of the 58 residue bovine pancreatic trypsin inhibitor containing between 21 and 27 alanine residues show cooperative two state folding with $\Delta H_{vH}/\Delta H_{cal} = 1$ and thermodynamics similar to the wild-type parent sequence which has 10 alanines (Fig. 1) [15]. Mutations were introduced at sites that were not essential for specifying tertiary structure and the disulphide bonds in BPTI were retained. Nevertheless, it is interesting that typical cooperative structure can still be specified with this simplified sequence.

It is clear from the DSC data for BPTI that the heat capacity level of the high temperature, denatured state is greater than that of the low temperature native state. This heat capacity change during unfolding (ΔCp_{D-N}) is large and positive and originates largely from the exposure of hydrophobic groups to solvent in the denatured state of the protein along with other minor contributions [16,17]. Its value can be measured directly from the DSC thermogram, but is more reliably determined by measuring ΔH_{cal} at a range of *Tm* values (usually by pH variation). From Eq. 1 it is evident that the ΔCp_{D-N} is the linear slope of the correlation between these two values.

The value of ΔCp_{D-N} could be determined for the BPTI mutants containing 21 and 22 alanines by varying the pH between 3.3 and 6.1 where the protein stability (*Tm*) changed (Fig. 1 lower panel). Values for the mutants were slightly lower than that of wild-type BPTI but this probably reflects the significant mutational change in these constructs (11 or 12 residues mutated to alanine). The

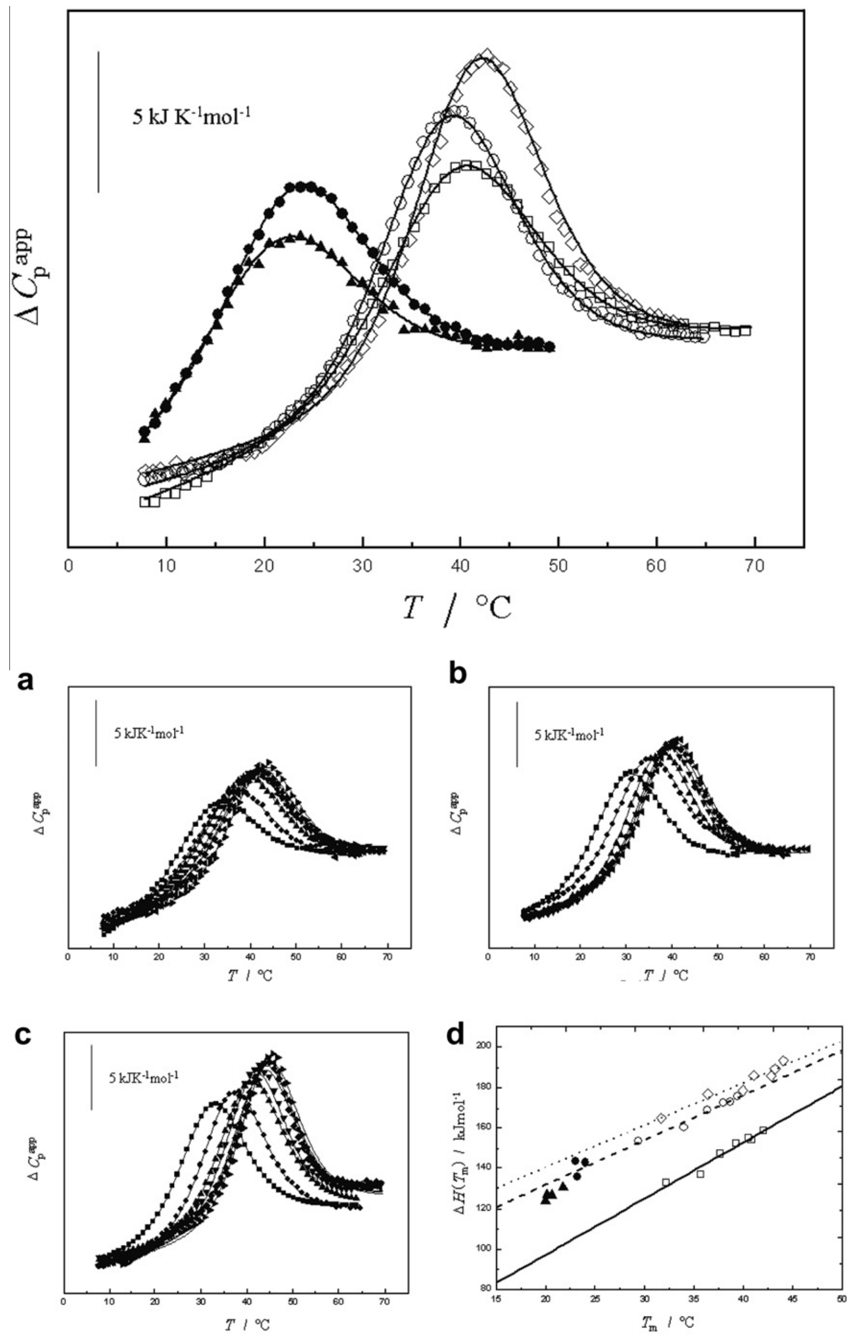

Fig. 1. Upper panel. DSC data for BPTI mutants (□) BPTI, (○) BPTI-21; (◇) BPTI-22; (●) BPTI-26; and (▲) BPTI-27. The numbers indicate the total number of alanine residues present in each construct. The continuous line shows the fitting assuming a two-state model with $\Delta H_{vH}/\Delta H_{cal}$ = 1.0 ± 0.1. Scan rate 1 °C/min, protein 1 mg/ml, buffer 20 mM acetate pH 4.7. Lower panels show the pH dependence of DSC thermograms for (a) BPTI, (b) BPTI-21 (c) BPTI-22 and (d) the fitted enthalpies as a function of Tm plotted to obtain values of ΔCp_{D-N}. Adapted from [15].

broad agreement supports the conclusion that the simplified proteins are folded and cooperative structures with properties similar to the parent BPTI. In contrast, the molten globule states of 4 different periplasmic binding proteins showed significant reductions of 30–70% in the value of ΔCp_{D-N} compared to the native protein. They still bound ligands and showed native like far-UV CD spectra but the reduction in ΔCp_{D-N} is consistent with a more 'dynamic' conformation in which hydrophobic groups are exposed to solvent [18].

The tetratricopeptide repeat (TPR) motif is another small protein of 34 residues that undergoes cooperative two-state unfolding with $\Delta H_{vH}/\Delta H_{cal}$ = 1 [19]. When linked as repeats, TPRs form non-globular structures stabilised by local short-range interactions with few long-range contacts. Changing the linker sequence, increasing the number of repeats from 2 up to 10 or varying the pH resulted in deviation from two-state unfolding as measured by DSC. This indicates that cooperativity is likely a subtle balance between local and longer range stabilising interactions between TPR domains [19,20]. Such effects have been studied in detail using a chimeric fusion protein of ubiquitin (Ubq) and the ubiquitin interacting motif (UIM) from VPS27p [21]. The ~20 residue UIM sequence was joined to the C-terminus of Ubq with linkers of varying length. The Tm of the fusion proteins was increased by at least 10 °C consistent with the formation of helical structure in the UIM sequence and its interaction with Ubq as seen in the NMR structure [22]. Global fitting of DSC and CD data revealed cooperative two-state thermal unfolding for all linker lengths. Mutations known to destabalise UIM, Ubq or the UIM-Ubq interface were also introduced separately, and only in the case of the loss of interface interactions was any reduction in cooperativity observed [21]. In an earlier study, chimeric fusions of the alpha-spectrin SH3 domain with a proline rich decapeptide ligand were studied using a similar combination of DSC, CD and NMR [23]. The fused protein was more stable than the parent SH3 domain, again consistent with the NMR structure that had showed normal binding of the tethered peptide [24]. This stabilisation was reduced on mutating each of the six proline residues in the fused peptide to alanine, thereby probing interface interactions. DSC data could be adequately fit to a two-state model but a global three-state analysis was used to fit the DSC data from which the weak affinities of the SH3-peptide interaction could be determined [23]. These subtle effects were in broad agreement with other estimates of affinity suggesting that the use of DSC and chimeric fusions could be a useful strategy for studying weak interactions.

Where thermal unfolding mechanism becomes more complex there are usually indicators from other biophysical measurements as well as DSC data that give progressively worse agreement between ΔH_{vH} and ΔH_{cal} or poor residuals where a two-state mechanism is assumed. Eventually it becomes obvious that a two-state model is inappropriate as there is more than one endothermic heat adsorption peak in the thermograms. DSC is extremely sensitive to such changes as the calorimeter is measuring directly the excess heat capacity of the process itself rather than a property, such as a spectroscopic signal, that may or may not change during denaturation. Thermal denaturation methods that follow ensemble properties of the states present produce a sigmoidal curve in which deviations from a single unfolding event are harder to discriminate and fit. Shoulders in the peaks of DSC thermograms and eventually distinct peaks are easily resolved in DSC data.

Such discrimination is evident in another chimeric fusion study where the unfolding of the linked proteins, FKBP12 and the FRB domain from mTOR, remain distinct; although there is some destabilisation of the FKBP12 from the coupling [25]. Unfolding of FKBP12 in the chimaera could be easily identified by adding the known ligand, FK506, resulting in a significant stabilisation of one peak with no effect on the other. Finally, adding rapamycin, which binds to both proteins, produced a ternary complex that unfolded with a single cooperative peak in the thermogram. The fusion strategy was partly motivated to improve the expression and stability of FRB for NMR studies, but the ability to selectively stabilise independently folded proteins or domains in such fusions shows the potential application of DSC in ligand identification.

Trigger factor is an important molecular chaperone binding to the exit tunnel from the 50 S ribosome subunit and has both a three domain structure (N, M and C domains) as well as being a dimer. DSC studies on the E.coli protein reveal independent unfolding of the three domains in the intact protein via intermediates that remain dimeric (Fig. 2) [26]. The C-terminal domain mediates the stabilisation of these dimeric intermediates, since its removal, in an NM domain construct, results in unfolding through only monomeric states. The crystal structure of this protein indicates dimer contacts between both N and C domains but DSC reveals that those between the C domains are the more important in dimer stabilisation during thermal denaturation [26]. The denaturation of this system was fitted to models in which the native state and intermediates were dimeric while the denatured state was considered monomeric. Such changes in molecularity during denaturation will cause the stability (*Tm*) to be dependent on protein concentration. If the native state has the higher degree of association, *Tm* increases with concentration, while if the denatured state is associated, as with aggregation, the *Tm* will decrease with concentration. DSC is a simple tool to test for these effects and

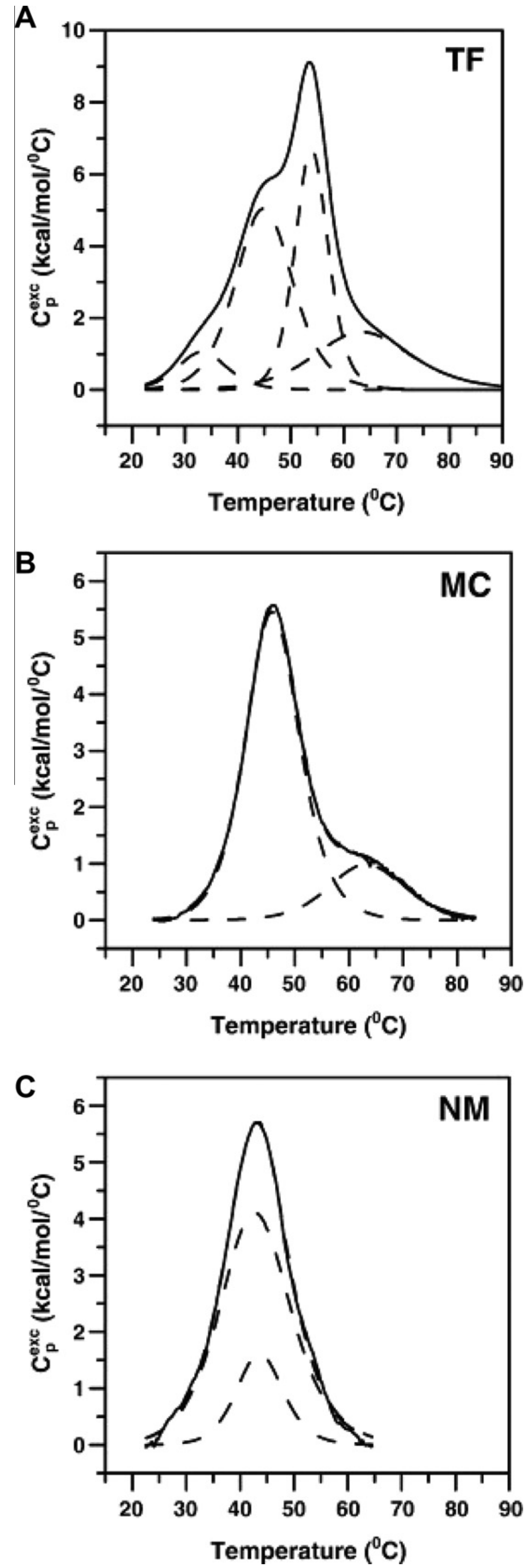

Fig. 2. DSC data for (A), full length Trigger factor, (B), mid and C-terminal domain construct and (C), N- and mid-domain construct. Protein concentration was 1 mg/ml. Scan rate 1 °C/min, buffer 10 mM sodium phosphate, pH 7.8. Reproduced from [26].

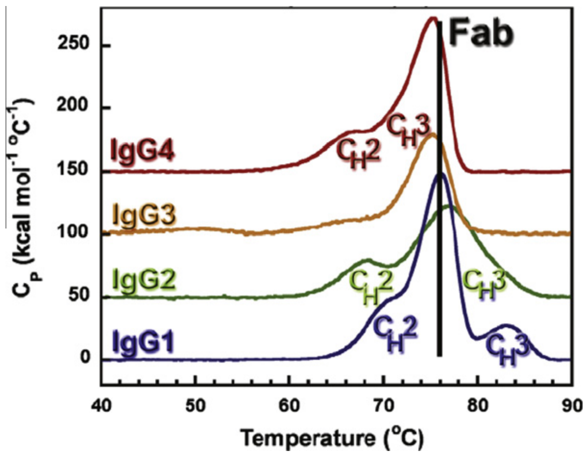

Fig. 3. DSC curves representing the four human IgG subclasses. A single line is drawn through the Fab unfolding transitions of each IgG. The C_H2 and C_H3 unfolding transitions of IgG1, IgG2, and IgG4 are labelled. Protein concentration was 1 mg/ml. Scan rate 1 °C/min, buffer 20 mM sodium citrate, 150 mM NaCl buffer at pH 6.0. Reproduced from [33].

the heat capacity profile can be fit to increasingly complex models with intermediate states that may or may not remain associated during denaturation [27–30]. In contrast, DSC of alpha-crystallin, which forms large heterogeneous oligomers, showed no dependence of stability on protein concentration supporting the argument that the denatured state retained the same level of association as the native protein [31].

Trigger factor is some 430 residues in size and it is common that larger proteins such as this are assembled from smaller domains that often unfold independently in a non–cooperative manner. The antibody IgG is a well studied example of such a protein where differing stabilities of the Fab domain and of the CH2 and CH3 domains of the Fc region can lead to up three distinct DSC peaks (Fig. 3) [32,33]. The stability of individual IgG domains can be modulated without affecting the others, for example through introduction of intradomain disulphides bonds in CH3 [34]. DSC was used to study the Trastuzumab-DM1 antibody-drug conjugate and was again able to demonstrate which domain, in this case CH2, was selectively destabalised by the DM1 moiety [35].

The denaturation of IgG is harder to analyse quantitatively as, unlike trigger factor, the process is not a reversible equilibrium. Irreversibility is a common feature of DSC measurements on larger proteins and limits the use of a standard equilibrium thermodynamic analysis. The irreversibility arises from many sources. Aggregation can be easily checked for by either performing standard absorbance tests for particle scattering or by simply visually examining the material after cooling and removal from the DSC cell. Chemical modifications, such as deamidation, can be verified by mass spectrometry. For irreversible denaturation the enthalpy and *Tm* become apparent values and should be indicated as such. Both parameters become dependent on scan rate and also usually on protein concentration reflecting the change in molecularity in the aggregating denatured state. Irreversibility may be avoided by working at low protein concentration and scanning relatively fast (up to 3 °C/min) since the kinetics of the irreversible processes are competing with the kinetics of the denaturation equilibrium. DSC can be used to analyse the irreversible kinetics. The simplest models consider only native protein and an irreversibly modified denatured state in a quasi two-state equilibrium (Scheme 1). More complex analysis treats the denaturation as an equilibrium between native and denatured protein which aggregates in an irreversible kinetic step [36].

$$N \xleftrightarrow{K_{D-N}} D \xrightarrow{k} Ag$$

Scheme 1.

Extrapolation of the kinetics allow estimates of protein kinetic stability at lower temperatures as might be encountered *in vivo* in the cell or *in vitro* on storage [37]. Proteolytic enzymes have even been included during DSC measurement in an attempt to probe kinetic stability under harsher conditions experienced by partially folded or unfolded conformations *in vivo* [38].

5. DSC and fast protein folding

There is continued interest in the ultra fast folding of small protein domains that fold and unfold on a microsecond timescale near theoretical speed limits for the process and on a time regime that is increasingly accessible to computer simulations. It might be initially surprising that an equilibrium technique such as DSC could contribute to studies on such rapidly folding systems, but the fundamental nature of the DSC measurement makes it intimately related to the protein unfolding partition function so that it can, in principle, be used to extract information about the folding free energy surface and the heights of energetic barriers.

Downhill protein folding over small or negligible energetic barriers was proposed as a prediction of landscape theory under conditions of extreme native bias [39]. Folding is then characterised by a simple diffusive search across an energy landscape without significant barriers. This scenario is clearly a natural extension of conventional barrier limited folding model in which a high-energy transition state represents the major barrier to folding. The height of the transition state barrier is variable for different proteins; reflected in their wide range of folding rates. For individual proteins, the folding barrier changes with different physical conditions such as temperature or denaturant, as seen, for example, in chevron plots of the denaturant-dependence of unfolding and folding rate constants. Thus if this barrier is variable, there could be certain conditions when it is insignificant compared to inherent thermal energy.

It has been suggested that some proteins may remain in a downhill folding regime under all equilibrium conditions in so a called ‘one-state’ or ‘global downhill folding’ mechanism [40]. In this scenario there is a single ensemble of structures present under any one set of conditions and the average properties of this ensemble are modulated between native and denatured like structures in a continuous manner as conditions change. This behaviour provides the attractive possibility of characterising the entire folding process at high resolution using an equilibrium technique such as NMR [41]; although such data have been questioned [42,43]. It has also been suggested that global downhill folding has a biological role allowing proteins to act as continuously variable structures in the form of a ‘molecular rheostat’ [40,44,45].

The proponents of one state folding have developed the use of DSC measurement to extract simplified one-dimensional representations of the free energy folding landscape and thus barrier heights [46]. In their original work they defined the unfolding enthalpy as an order parameter and represented the free energy landscape as quartic polynomials used in Landau’s theory of critical phase transitions [46]. More recently they have extended the analysis to use structure based order parameters as well as analysing combinations of their methods [47]. In these cases they claim that unfolding of a small helical protein which is the peripheral subunit binding domain from the 2-oxo- glutarate dehydrogenase multienzyme complex (BBL from *Escherichia coli* and PDD from *Bacillus stearothermophilus*) as well as the alpha–beta head stabilising protein from bacteriophage lambda (gpW), all occur over minor barriers,

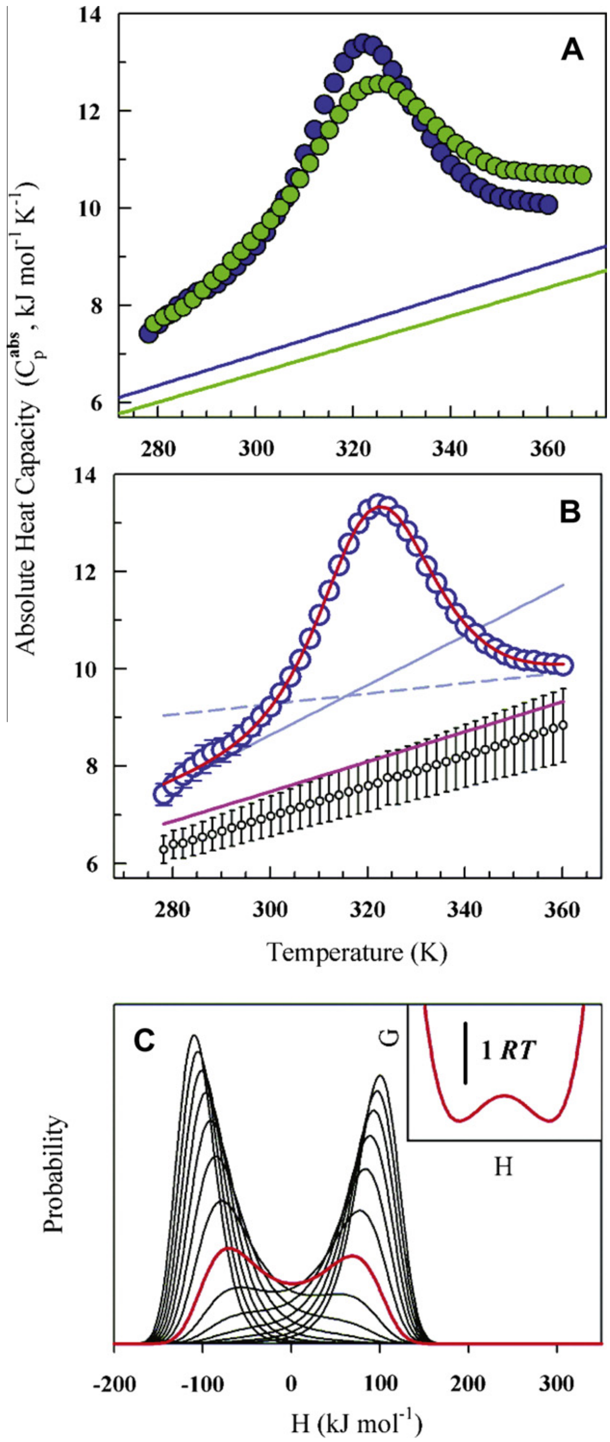

Fig. 4. DSC of PDD (blue) and BBL (green). (A) Direct comparison of the absolute heat capacity of the two proteins (circles) plotted with the Freire's empirical native baselines [14]. (B) The best fit of the PDD data (open circles) to the variable barrier model (red curve) together with the fitted native baseline (magenta). Freire's native baseline with the error estimated from experiments at various protein concentrations is shown for comparison (black symbols). The gray dashed and continuous lines are the unfolded and folded baselines, respectively, obtained from a two-state fit. (C) The probability density from the best fit to the variable barrier model (black curves). The red distribution is the corresponding probability density at $T_0 \approx 323$ K. (inset) Free-energy surface at T_0 obtained from the best fit. Reprinted with permission from A.N. Naganathan, P. Li, R. Perez-Jimenez, J.M. Sanchez-Ruiz, V. Munoz, Journal of the American Chemical Society 132 (2010) 11183–11190. Copyright 2010 American Chemical Society.

on the order of RT in magnitude, in the 'downhill folding regime' or as 'global downhill folders' (Fig. 4) [47,48].

Much importance is attached to the value and slope of the absolute heat capacity for the native state (or low temperature region) of the thermograms from these putative one-state folding proteins when compared with 'universal' values and slopes in the literature [14]. The level of heat capacity and its dependence on temperature are both higher than expected and classed as 'unphysical' [46]. It is of note that the 'universal' values used as reference data were originally recorded in the 1990's (although re-measured and added to in recent work) and consequently include a large proportion of commercially available proteins which, through ease of availability, were often extracellular proteins with between one and five disulphide cross links (>50% of the original sample group [14]). DSC measurements were made under oxidising condition with these crosslinks formed in both native and denatured states. Such a data set may not be completely appropriate for the smaller protein domains that are the subject the downhill folding work. These proteins lack disulphides and, in the case of BBL and PDD, have been excised from their natural context in large intracellular proteins assemblies.

There are a number of factors that might give atypical native state heat capacity in DSC baselines. Incorrect or inadequate sample preparation can be excluded, as the authors are established experts in the DSC field. However, the slope of the low temperature baselines in DSC thermograms of 10 different DNA binding domains that have been studied has been noted to be above the 'universal' value to a similar extent as the downhill folding proteins [8,47]. This observation has been attributed to the distinctly flexible structures of these domains that enable them to bind DNA, rather than to any downhill folding behaviour; presumably because their folding rates are also in some cases sufficiently slow to preclude such a claim. The unfolding of the DNA binding homeodomain from the human transcription factor PBX has recently been studied in greater depth using a combination of DSC and NMR thermal denaturation [49]. The DSC thermogram shows a steeply sloping native state baseline that can be fitted using the Landau model to predict that there was no barrier between the native and denatured states. The protein folds on a microsecond time scale in support of this conclusion. However, global analysis of the DSC and NMR data and cross validating them with NMR relaxation dispersion experiments showed the coexistence of distinct folded and denatured forms of the protein present at temperatures well below the transition region [49]. Large-scale structural and dynamic changes in the native state of PBX were also observed, indicating significant flexibility and in line with the conclusions on other DNA binding proteins.

A major difficulty in studying small proteins by DSC is a correspondingly small enthalpy of unfolding which produces deceptively broad unfolding transitions that can easily merge with the perceived native baseline region and give it an artificially high slope (for example BPTI mutants in Fig. 1). These small proteins are also often only marginally stable: even at temperatures of maximum stability their equilibrium may be only a few kcal/mol. As a result there is a risk that the native state may never be fully populated and the presence of low levels of denatured material present (in a two-state equilibrium scenario) will elevate the observed heat capacity in low temperature regions as seen for PBX [49]. This effect can be exacerbated by structured denatured states, or structured intermediates, (again in a barrier limited folding scheme), which typically have strongly sloping DSC thermograms at lower temperatures as seen for BBL and other members of the peripheral subunit binding domain family [50–52]. Overall, such complicating factors do not detract from the validity of the novel analytical approaches to DSC data, but add considerable complexity that must be considered.

A variable barrier model has also been applied to DSC data for the catalytically promiscuous isoform of glutathione S-transferase, GSTA1–1, where an additional low temperature shoulder unique to this isoform is seen [53]. This event has been linked to 'repacking' of the C-terminal helix, rather than any unfolding of the protein, using a combination of ligand binding, mutation, and CD studies. Analysis of the isolated low temperature transition, once deconvolved from the DSC scan, appears to indicate that the proposed conformational sampling of the folded C-terminal helix around the active site occurs without a significant free energy barrier while unfolding of the remainder of the protein at higher temperature occurs with large defined barriers. This dynamic flexibility could facilitate the enzyme's promiscuity at its functional temperature when compared with other substrate specific isoforms that lack the low temperature shoulder [53]. It would be interesting to see whether the kinetics of these helix motions are consistent with such a barrierless regime and why this flexibility is associated with such large heat adsorption seen by DSC.

DSC of the GYF domain from human CD2BP2 is another case where unusual properties are seen for native and denatured state heat capacity levels in a small marginally stable protein [54]. Data from DSC and CD thermal denaturation were fit to a global two-state equilibrium model for this protein and so it will be interesting to see on what time scale its folding kinetics eventually indicate in terms of classifying its mechanism. Indeed, it will be interesting to examine more widely the robustness and practical utility of the various methods in extracting barrier heights from DSC data when, as published (URL in [47]), the appropriate programs are made available to the scientific community as web applications. DSC data are already to hand for small proteins that fold slowly and mutants of faster folding proteins that alter significantly their folding rate [55]. These will be prime candidates for testing these methods.

The nature and magnitude of protein folding energy barriers and subtle, often semantic, distinctions between downhill folding under certain conditions as opposed to true 'one-state' folding will no doubt continue to occupy space in the literature. Disagreements between various groups may reflect the effects of the small differences in construct length used for BBL, the buffer and pH and the use or not of extrinsic fluorophores [56–58]. Indeed, even single molecule FRET based measurements, which can categorically resolve ensemble heterogeneity in BBL into discrete native and denatured states separated by a significant energy barrier have proved controversial [59,60]. However, the real importance of downhill folding scenarios, and one-state folding, should it occur, will be in their contribution to our understanding of folding mechanism and a demonstration of their claimed function as molecular rheostats in the biological systems from which these small experimental proteins are obtained.

6. DSC and protein stability

Protein thermal 'stability' often has two components; equilibrium and kinetic, both of which can be quantified using DSC as discussed above. DSC also measures basic thermostability, or 'susceptibility', of proteins to thermal denaturation as reflected in the measured *Tm* of the thermogram. This *Tm* may by an equilibrium thermodynamic value or an apparent one in the case of irreversible denaturation. It is important not to confuse measured thermostability with the level of equilibrium stability at lower temperatures relevant to physiological or experimental conditions. The equilibrium stability of two proteins with similar *Tm* may be quite different at lower temperatures if their values of $\Delta Cp_{\mathrm{D-N}}$ are dissimilar. Extrapolation of equilibrium stability away from the Tm, where the stabalising free energy ($\Delta G_{\mathrm{D-N}}$) is zero for a simple reversible system, requires the measured $\Delta H_{\mathrm{D-N}}$ and $\Delta Cp_{\mathrm{D-N}}$ in standard equations

$$\Delta G_{\mathrm{D-N}} = [\Delta H_{\mathrm{D-N}} + \Delta Cp_{\mathrm{D-N}}(T - Tm)] - T\left[\frac{\Delta H_{\mathrm{D-N}}}{Tm} + \Delta Cp_{\mathrm{D-N}} \ln\left(\frac{T}{Tm}\right)\right] \tag{3}$$

Simple simulations, using typical values for *Tm* and $\Delta H_{\mathrm{D-N}}$ but different values of $\Delta Cp_{\mathrm{D-N}}$, can reveal the effect of this property on the profile of the $\Delta G_{\mathrm{D-N}}$ function in terms of its magnitude, temperature of maxima and the predicted temperature for cold denaturation of the system.

DSC has the advantage of being a universal method for studying thermal denaturation. It has no reliance on changes in spectroscopic signal, such as in CD or fluorescence based thermal denaturation, and since it measures directly the heat absorption associated with the process it is more capable of resolving multiple overlapping processes as noted above. DSC is normally measured with a small excess pressure applied to the sample and reference cell which permits scans of up to 140 °C or so on aqueous systems without the sample boiling. This ability is particularly useful for studying proteins isolated from thermophilic and hyperthermophilic organisms, many of which have melting temperatures well above 100 °C [61,62]. How this stability is achieved (via equilibrium or kinetic mechanisms) and particular sequence and structural features conferring enhanced thermostability are clearly of great interest for biotechnology applications [63,64]. DSC is the method of choice since a full thermodynamic characterisation can reveal the temperature dependence of the thermal equilibrium and thus the mechanism by which thermostability is achieved. Changes to the stability curve that achieve this could be simply increasing equilibrium stability at lower temperatures (upward shift), increasing the temperature of maximum stability in the curve (rightward shift) or a reduction in $\Delta Cp_{\mathrm{D-N}}$ producing a broadening of the stability curve (flattening shift) [65]. Practical and theoretical approaches to increasing thermostability could be guided by the observed design rules of natural thermophiles, or those obtained during laboratory selection [65–68]. The use of paleogenetics to reconstruct thioredoxin enzymes from extinct organisms has also revealed remarkable increases in thermostability. The Tm of these ancestral sequences was ~25 °C higher than modern *E. coli* or human thioredoxin consistent with progressive cooling of the environment by this amount over the ~5 billion year period of evolution [69,70].

More generally, the *Tm* of a protein is an established parameter that can indicate other useful properties of proteins such as their likelihood of successfully crystalising for high-resolution structural work [71] and their potential shelf life in a particular pharmaceutical formulation [72]. These correlations reflect the fact that populating the native state is essential, providing the chance for ordered crystal packing and growth, and that the denatured state or unfolding intermediates are the most common sources of material for irreversible processes, such as aggregation, that lead to loss of function.

It is established that conditions, or stabilising additives, that increase *Tm* are useful parameters to optimise for success in crystalisation [71,73]. Indeed, increasing *Tm* through mutagenesis is part of the core strategy implemented in commercial technology offered by Heptares to facilitate structure determination for GPCR proteins (StaR technology$^{\mathrm{TM}}$). In high throughput methods for measuring protein *Tm* the most common techniques use a fluorescent reporter dye (Sypro orange) that increases fluoresecence on interaction with the hydrophobic groups that are normally buried in the protein core and is thus an indicator of unfolding. These differential scanning fluorimetry (DSF) experiments are implemented in parallel in a plate format or in a spinning rotor. Values of *Tm* from DSF have been shown to correlate well with those seen in DSC. The absolute values from DSF are systematically lower, possibly reflecting a destabilising effect of the reporter dye or problems with the method of fitting to *Tm* [72]. Recent work has shown that although DSC may lack the throughput of fluorescence based methods, it may have an advantage in measuring both *Tm* and enthalpy as the area and breadth of the enthalpic heat absorption peak may be used as additional indicators for successful crystal growth [74].

Biopharmaceutical formulation is another important aspect of protein stability that is of interest because of the increasing numbers of protein-based therapeutics. These are often administered by injection as small volumes of highly concentrated solution and so must be prepared under conditions where the active protein can be stored without degrading. Aggregate formation is particularly problematic as these species may be immunogenic or toxic [75,76]. Buffer, ionic strength, pH, protein concentration and additives such as sugars, polyols, amino acids, surfactants, anti oxidants etc., are all variables that need to be optimised on a case-by-case basis [77–80]. Similarly, covalent modifications to the protein such as glycosylation and PEGylation have variable consequences on protein thermal stabilities [81–84]. Protein storage may also be enhanced by the exclusion of water by a variety of methods; freeze drying being the most common. DSC can contribute to the development of these processes [85,86] and to the assessment of the viability of the protein on dissolving back into solution [87]. DSC is one of main techniques used to assess thermal stability of formulations, often in combination with DSF and other analytical methods using temperature, with the apparent *Tm* obtained being a key indicator of desirable shelf life. Combinations of biophysical techniques are most informative as additives can have contrasting effects on the equilibrium component of the thermal denaturation and the kinetics of the irreversible processes (Scheme 1) as seen for IgG [88,89].

The excipients used in formulation typically affect the ability of the protein to self associate through indirect effects on the solvent, but in some cases they can act to stabilise the system by binding directly to the native state of the protein. Ligands will increase the stability of the binding competent state by shifting the equilibrium position in simple mass action effect and if this stabilisation can be measured, for example in an increasing *Tm* shift, then it is possible to extract the binding affinity of the ligand itself. Analysis of DSC data in this way is well established and can potentially quantify extremely tight binding affinities [90,91].

Changes in the *Tm* on ligand binding can be quite large. The *Tm* of the metalochaperone Sco is increased by 23 °C on binding Cu(II), corresponding to an Kd of 3.5 pM [92]. Similarly, binding of a range of clinical and experimental inhibitors of HIV protease increased the *Tm* of the protein by between 6 and 22 °C corresponding to nM or tighter affinity when extrapolated from the *Tm* to 25 °C [93]. Although the agreement between the absolute affinities calculated at 25 °C and those determined directly by ITC was not good, the relative differences in affinities between inhibitors was well reported. Similarly, two mutants in the protease active site (D25N and D29N) showed significantly weaker inhibitor binding as reflected in the smaller *Tm* shifts observed compared to wildtype [93].

7. DSC of complex samples

The formation of amyloid like aggregates seems to be a somewhat generic property of most polypeptide sequences given sufficient time and appropriate conditions [94]. Their association with a number of important pathological conditions has generated huge interest in this area of protein chemistry. Although they share a number of common structural and biochemical properties, such as specific dye binding, high beta-sheet content and fibrillar architecture, they have diverse gross morphology, even within an individual sample formed from a common stock solution of soluble protein. Despite this challenging complexity, amyloid material from a number of proteins have been studied by DSC. Remarkably, the amyloid fibrils formed from a mutant of the alpha-spectrin SH3 domain displayed a simple single heat adsorption peak in DSC thermograms (Fig. 5) [95]. It is evident that the heat capacity of the low temperature fibre state is higher than the native monomeric protein while the enthalpy and the $\Delta Cp_{\mathrm{D-N}}$ of denaturation are both smaller. These features are all consistent with the view that amyloid fibrils are composed of extended and partially structured protein monomers with a high level of hydration in comparison to the native globular SH3. The stability of the fibrils was dependent on concentration but not affected by the instrumental scan rate suggesting that in this case the melting process was a 'quasi-equilibrium' and not under kinetic control of reversible processes. Based on this a simple equilibrium polymerisation model could be applied to the DSC data with some success [95].

In contrast to this surprising simplicity, DSC studies of amyloid formed from beta 2- macroglobulin and hen egg white lysozyme are complex [96,97]. Material in these studies was primed for amyloid formation by stirring for 24 h at 37 °C and then the amyloid formed during the process of heating in the DSC itself. The morphology and homogeneity of the fibrils and their thioflavin T binding suggested mature amyloid, but the DSC scans of this material, in rescans of the initial amyloid forming scan, showed only exothermic heat effects with a dominant kinetic effects. The material produced during the stirring phase was heterogeneous smaller aggregates, yet the formation of amyloid was completely dependent on this stirring; even to the extent of the stirring speed and geometry of the vessel used [96]. Such variability reflects the complexity of the seeding, nucleation and growth mechanisms of amyloid material which must be standardised on a protein-by-protein case.

Another recent development in the field of DSC has been its application to the analysis of complex biological samples, such as blood plasma, with the goal of disease diagnosis [98,99]. Human plasma is an incredibly complex mixture of protein and small molecule components with over 1000 proteins identified from proteomic technologies. DSC is able to measure the complex thermogram of this mixture when diluted down to a few of mg/ml total protein with the resultant profile representing the weighted sum of the abundance of individual components and their thermal stabilities. The majority of the signal comes from the 10 or so major protein components of plasma and the 'average ' measured plasma thermogram can be regenerated from individual DSC scans of these purified proteins combined and weighted according to their established levels in human plasma (Fig. 6) [99]. The heat capacity measured in a DSC experiment is an extensive property of a protein solution and so works reflecting the concentrations in this manner.

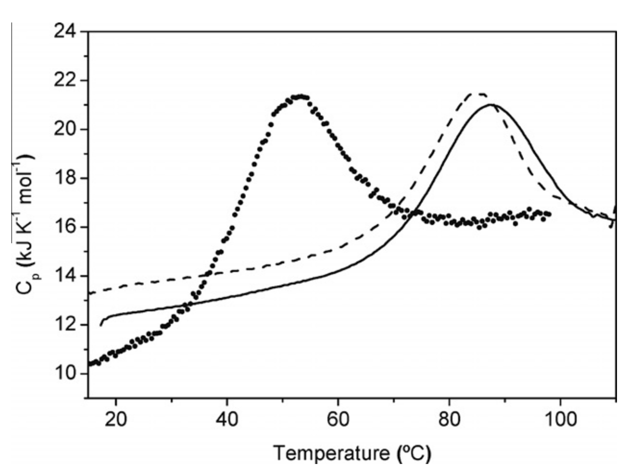

Fig. 5. DSC data for amyloid fibrils of N47A Spc-SH3. Fibrils prepared by 1 month of incubation at 37 °C and resuspended at 6 mg mL^{-1} (solid line). Fibrils prepared by 10 days of incubation at 37 °C and resuspended at 7.5 mg mL^{-1} (dashed line). Soluble native protein at 1.8 mg mL^{-1} (dots). Reprinted with permission from B. Morel, L. Varela, F. Conejero-Lara, The Journal of Physical Chemistry. B 114 (2010) 4010–4019. Copyright 2010 American Chemical Society.

However, the excellent agreement between the simulated and observed thermograms indicates that the proteins do not seem to self-assosciate or interact with each other and behave as a somewhat 'ideal' solutes in the plasma mixture.

Established differences in the levels of the major plasma proteins arising from demographic factors such as gender and ethnicity could be detected in the DSC thermograms of 'healthy' individuals. However, the remarkable observation of this work is that the plasma thermograms obtained from individuals suffering from a range of diseases is quite unique. Each disease seems to present a 'fingerprint' thermogram that is distinct from the normal healthy plasma thermogram and that of the other diseases examined to date (Fig. 7) [98].

These changes seem to shift the envelope of heat absorption toward higher temperature and since it is established that the levels of the major plasma proteins do not change significantly during these diseases, the authors speculate that the changes in the thermograms arise through the stabilisation of these proteins by binding biomolecule ligands which are produced in the circulation during the disease process. This pool of ligands, termed the "interactome" could include unusual metabolites or breakdown products from unnatural cellular processes or infections. In support of this conclusion the authors have demonstrated that the changes in the plasma profile similar to those seen in disease can be mimicked by the deliberate addition of know ligands for human serum albumin; the main component of plasma. Control measurements also showed that the stability of purified human serum albumin was stabilised by similar levels with increases in *Tm* up to 10 K [98].

This application of DSC is another example of the technique's use to reveal changes in stability as a result of ligand binding, as discussed earlier. Although the ligands causing stabilisation are currently unknown, the complex nature of plasma and resultant additive shape of the plasma thermogram seem to make it

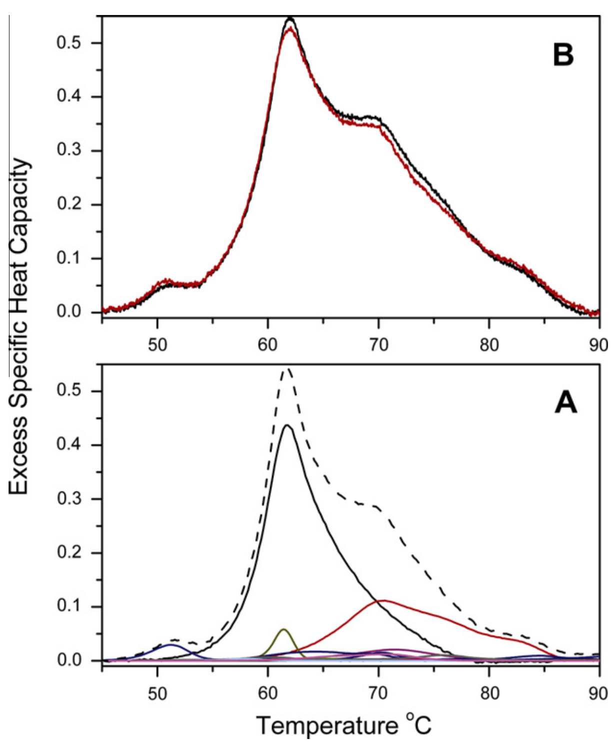

Fig. 6. DSC thermograms of human plasma (A) calculated thermogram (*dashed line*) obtained from the sum of the weighted contributions of the 16 most abundant plasma proteins. (B) Thermograms obtained from mixtures of pure plasma proteins, mixed at concentrations that mimic their known average concentrations in normal plasma. The red curve is a mixture of HSA, IgG, fibrinogen, and transferrin. The black curve is a mixture of the 16 most abundant plasma proteins. Reproduced from [99].

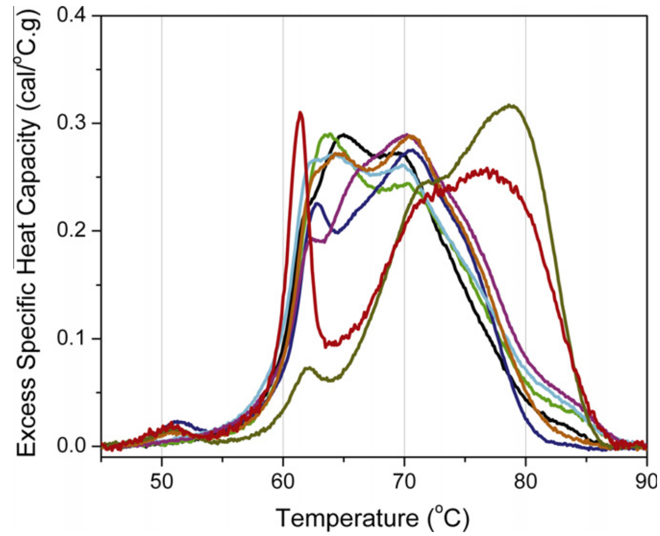

Fig. 7. Average DSC thermograms for individuals diagnosed with various cancers and diseases. Endometrial cancer (black line; duplicate DSC runs on samples from 8 individuals); amyotrophic lateral sclerosis (green line; duplicate DSC runs on samples from 12 individuals); lung cancer (blue line; duplicate DSC runs on samples from 30 individuals); ovarian cancer (cyan line; duplicate DSC runs on samples from 12 individuals); lyme disease (dark yellow line; duplicate DSC runs on samples from 4 individuals); systemic lupus erythematosus (red line; duplicate DSC runs on samples from 2 individuals); rheumatoid arthritis (orange line; duplicate DSC runs on samples from 5 individuals); melanoma (magenta line; duplicate DSC runs on samples from 5 individuals). Reproduced from [98].

remarkably sensitive to them. Some of the latest work from these authors has even shown that the plasma thermogram may be able to distinguish different stages of the progression of a disease such as carcinoma of the cervix [98]. This raises the distinct possibility that DSC might become a routine method for screening, early diagnosis and disease monitoring in clinical labs.

This 'frontier spirit' to DSC is being used by other groups and has not stopped with plasma. Other clinical samples such as urine, saliva and cerebrospinal fluid have also been examined [100–102]. The typical content of these samples is less well documented than plasma and so it is more difficult to confirm the basis of the observed thermograms measured. Nevertheless, this will undoubtedly be an area for development as the principals applied to plasma become more established in the literature.

References

[1] W.M. Jackson, J.F. Brandts, Biochemistry 9 (1970) 2294–2301.
[2] P.L. Privalov, N.N. Khechinashvili, B.P. Atanasov, Biopolymers 10 (1971) 1865–1890.
[3] J.M. Sturtevant, Annual Review of Biophysics and Bioengineering 3 (1974) 35–51.
[4] R. Biltonen, A.T. Schwartz, I. Wadso, Biochemistry 10 (1971) 3417–3423.
[5] S.J. Gill, K. Beck, The Review of Scientific Instruments 36 (1965) 274–276.
[6] V. Plotnikov, A. Rochalski, M. Brandts, J.F. Brandts, S. Williston, V. Frasca, L.N. Lin, Assay and Drug Development Technologies 1 (2002) 83–90.
[7] V.V. Plotnikov, J.M. Brandts, L.N. Lin, J.F. Brandts, Analytical Biochemistry 250 (1997) 237–244.
[8] P.L. Privalov, A.I. Dragan, Biophysical Chemistry 126 (2007) 16–24.
[9] C.H. Spink, Methods in Cell Biology 84 (2008) 115–141.
[10] C. Demetzos, Journal of Liposome Research 18 (2008) 159–173.
[11] S.E. Permyakov, Methods in Molecular Biology 896 (2012) 283–296.
[12] A. Cooper, M.A. Nutley, A. Wadood, in: B.Z.C.S.E. Harding (Ed.), Protein–Ligand Interactions: hydrodynamics and calorimetry, Oxford University Press, Oxford, New York, 2000, pp. 287–318.
[13] V. Kholodenko, E. Freire, Analytical Biochemistry 270 (1999) 336–338.
[14] J. Gomez, V.J. Hilser, D. Xie, E. Freire, Proteins 22 (1995) 404–412.
[15] A. Kato, M. Yamada, S. Nakamura, S. Kidokoro, Y. Kuroda, Journal of Molecular Biology 372 (2007) 737–746.
[16] J.M. Sturtevant, Proceedings of the National Academy of Sciences of the United States of America 74 (1977) 2236–2240.
[17] R.S. Spolar, J.H. Ha, M.T. Record Jr., Proceedings of the National Academy of Sciences of the United States of America 86 (1989) 8382–8385.

[18] R.S. Prajapati, S. Indu, R. Varadarajan, Biochemistry 46 (2007) 10339–10352.
[19] J.J. Phillips, Y. Javadi, C. Millership, E.R. Main, Protein Science. A Publication of the Protein Society 21 (2012) 327–338.
[20] A.L. Cortajarena, L. Regan, Protein Science. A Publication of the Protein Society 20 (2011) 336–340.
[21] M.M. Patel, N.G. Sgourakis, A.E. Garcia, G.I. Makhatadze, Biochemistry 49 (2010) 8455–8467.
[22] N.G. Sgourakis, M.M. Patel, A.E. Garcia, G.I. Makhatadze, S.A. McCallum, Journal of Molecular Biology 396 (2010) 1128–1144.
[23] A.M. Candel, N.A. van Nuland, F.M. Martin-Sierra, J.C. Martinez, F. Conejero-Lara, Journal of Molecular Biology 377 (2008) 117–135.
[24] A.M. Candel, F. Conejero-Lara, J.C. Martinez, N.A. van Nuland, M. Bruix, FEBS Letters 581 (2007) 687–692.
[25] M. Sekiguchi, Y. Kobashigawa, M. Kawasaki, M. Yokochi, T. Kiso, K. Suzumura, K. Mori, T. Teramura, Inagaki, Protein engineering, Design & Selection: PEDS 24 (2011) 811–817.
[26] D.J. Fan, Y.W. Ding, X.M. Pan, J.M. Zhou, Biochimica et Biophysica Acta 1784 (2008) 1728–1734.
[27] O. Boudker, M.J. Todd, E. Freire, Journal of Molecular Biology 272 (1997) 770–779.
[28] I. Burgos, S.A. Dassie, G.D. Fidelio, The Journal of Physical Chemistry. B 112 (2008) 14325–14333.
[29] C.R. Johnson, P.E. Morin, C.H. Arrowsmith, E. Freire, Biochemistry 34 (1995) 5309–5316.
[30] J. Murciano-Calles, E.S. Cobos, P.L. Mateo, A. Camara-Artigas, J.C. Martinez, Biophysical Journal 99 (2010) 263–272.
[31] T. Rasmussen, M. van de Weert, W. Jiskoot, M.R. Kasimova, Proteins 79 (2011) 1747–1758.
[32] R.M. Ionescu, J. Vlasak, C. Price, M. Kirchmeier, Journal of Pharmaceutical Sciences 97 (2008) 1414–1426.
[33] E. Garber, S.J. Demarest, Biochemical and Biophysical Research Communications 355 (2007) 751–757.
[34] G. Wozniak-Knopp, F. Ruker, Archives of Biochemistry and Biophysics (2012). 181–187.
[35] A.A. Wakankar, M.B. Feeney, J. Rivera, Y. Chen, M. Kim, V.K. Sharma, Y.J. Wang, Bioconjugate Chemistry 21 (2010) 1588–1595.
[36] J.M. Sanchez-Ruiz, Biophysical Journal 61 (1992) 921–935.
[37] J.M. Sanchez-Ruiz, Biophysical Chemistry 148 (2010) 1–15.
[38] G. Tur-Arlandis, D. Rodriguez-Larrea, B. Ibarra-Molero, J.M. Sanchez-Ruiz, Biophysical Journal 98 (2010) L12–L14.
[39] J.D. Bryngelson, J.N. Onuchic, N.D. Socci, P.G. Wolynes, Proteins 21 (1995) 167–195.
[40] M.M. Garcia-Mira, M. Sadqi, N. Fischer, J.M. Sanchez-Ruiz, V. Munoz, Science 298 (2002) 2191–2195.
[41] M. Sadqi, D. Fushman, V. Munoz, Nature 442 (2006) 317–321.
[42] N. Ferguson, T.D. Sharpe, C.M. Johnson, P.J. Schartau, A.R. Fersht, Nature 445 (2007) E14–E15. discussion E17–18.
[43] Z. Zhou, Y. Bai, Nature 445 (2007) E16–E17. discussion E17–18.
[44] A. Fung, P. Li, R. Godoy-Ruiz, J.M. Sanchez-Ruiz, V. Munoz, Journal of the American Chemical Society 130 (2008) 7489–7495.
[45] A.N. Naganathan, U. Doshi, A. Fung, M. Sadqi, V. Munoz, Biochemistry 45 (2006) 8466–8475.
[46] V. Munoz, J.M. Sanchez-Ruiz, Proceedings of the National Academy of Sciences of the United States of America 101 (2004) 17646–17651.
[47] A.N. Naganathan, R. Perez-Jimenez, V. Munoz, J.M. Sanchez-Ruiz, Physical Chemistry Chemical Physics: PCCP 13 (2011) 17064–17076.
[48] A.N. Naganathan, P. Li, R. Perez-Jimenez, J.M. Sanchez-Ruiz, V. Munoz, Journal of the American Chemical Society 132 (2010) 11183–11190.
[49] P. Farber, H. Darmawan, T. Sprules, A. Mittermaier, Journal of the American Chemical Society 132 (2010) 6214–6222.
[50] N. Ferguson, R. Day, C.M. Johnson, M.D. Allen, V. Daggett, A.R. Fersht, Journal of Molecular Biology 347 (2005) 855–870.
[51] N. Ferguson, T.D. Sharpe, P.J. Schartau, S. Sato, M.D. Allen, C.M. Johnson, T.J. Rutherford, A.R. Fersht, Journal of Molecular Biology 353 (2005) 427–446.
[52] E. Arbely, T.J. Rutherford, H. Neuweiler, T.D. Sharpe, N. Ferguson, A.R. Fersht, Journal of Molecular Biology 403 (2010) 313–327.
[53] M.T. Honaker, M. Acchione, J.P. Sumida, W.M. Atkins, The Journal of Biological Chemistry 286 (2011) 42770–42776.
[54] M. Andujar-Sanchez, E.S. Cobos, I. Luque, J.C. Martinez, The Journal of Physical Chemistry. B 116 (2012) 7168–7175.
[55] C.A. Dodson, N. Ferguson, T.J. Rutherford, C.M. Johnson, A.R. Fersht, Protein Engineering Design & Selection: PEDS 23 (2010) 357–364.
[56] E. Arbely, T.J. Rutherford, T.D. Sharpe, N. Ferguson, A.R. Fersht, Journal of Molecular Biology 387 (2009) 986–992.
[57] H. Neuweiler, T.D. Sharpe, C.M. Johnson, D.P. Teufel, N. Ferguson, A.R. Fersht, Journal of Molecular Biology 387 (2009) 975–985.
[58] J. Fan, M. Duan, D.W. Li, H. Wu, H. Yang, L. Han, S. Huo, Biophysical Journal 100 (2011) 2457–2465.
[59] F. Huang, L. Ying, A.R. Fersht, Proceedings of the National Academy of Sciences of the United States of America 106 (2009) 16239–16244.
[60] J. Liu, L.A. Campos, M. Cerminara, X. Wang, R. Ramanathan, D.S. English, V. Munoz, Proceedings of the National Academy of Sciences of the United States of America 109 (2012) 179–184.
[61] M. Sawano, H. Yamamoto, K. Ogasahara, S. Kidokoro, S. Katoh, T. Ohnuma, E. Katoh, S. Yokoyama, K. Yutani, Biochemistry 47 (2008) 721–730.
[62] K.A. Luke, C.L. Higgins, P. Wittung-Stafshede, The FEBS Journal 274 (2007) 4023–4033.
[63] Y. Matsuura, M. Takehira, M. Sawano, K. Ogasahara, T. Tanaka, H. Yamamoto, N. Kunishima, E. Katoh, K. Yutani, The FEBS Journal 279 (2012) 78–90.
[64] M. Olszewski, A. Grot, M. Wojciechowski, M. Nowak, M. Mickiewicz, J. Kur, BMC Microbiology 10 (2010) 260.
[65] M.Z. Kamal, S. Ahmad, P. Yedavalli, N.M. Rao, Biochimica et Biophysica Acta 1804 (2010) 1850–1856.
[66] F. Sterpone, S. Melchionna, Chemical Society Reviews 41 (2012) 1665–1676.
[67] R. Ruller, L. Deliberto, T.L. Ferreira, R.J. Ward, Proteins 70 (2008) 1280–1293.
[68] Y. Matsuura, M. Ota, T. Tanaka, M. Takehira, K. Ogasahara, B. Bagautdinov, N. Kunishima, K. Yutani, Journal of Biochemistry 148 (2010) 449–458.
[69] E.A. Gaucher, S. Govindarajan, O.K. Ganesh, Nature 451 (2008) 704–707.
[70] R. Perez-Jimenez, A. Ingles-Prieto, Z.M. Zhao, I. Sanchez-Romero, J. Alegre-Cebollada, P. Kosuri, S. Garcia-Manyes, T.J. Kappock, M. Tanokura, A. Holmgren, J.M. Sanchez-Ruiz, E.A. Gaucher, J.M. Fernandez, Nature structural & Molecular Biology 18 (2011) 592–596.
[71] F. Dupeux, M. Rower, G. Seroul, D. Blot, J.A. Marquez, Acta crystallographica. Section D, Biological crystallography 67 (2011) 915–919.
[72] F. He, S. Hogan, R.F. Latypov, L.O. Narhi, V.I. Razinkov, Journal of Pharmaceutical Sciences 99 (2010) 1707–1720.
[73] U.B. Ericsson, B.M. Hallberg, G.T. Detitta, N. Dekker, P. Nordlund, Analytical Biochemistry 357 (2006) 289–298.
[74] F.H. Niesen, A. Koch, U. Lenski, U. Harttig, Y. Roske, U. Heinemann, K.P. Hofmann, Journal of Structural Biology 162 (2008) 451–459.
[75] M. Vazquez-Rey, D.A. Lang, Biotechnology and Bioengineering 108 (2011) 1494–1508.
[76] S. Hermeling, H. Schellekens, D.J. Crommelin, W. Jiskoot, Pharmaceutical Research 20 (2003) 1903–1907.
[77] S. Bai, M.C. Manning, T.W. Randolph, J.F. Carpenter, Journal of Pharmaceutical Sciences 100 (2011) 836–848.
[78] S.B. Hari, H. Lau, V.I. Razinkov, S. Chen, R.F. Latypov, Biochemistry 49 (2010) 9328–9338.
[79] E. Sahin, A.O. Grillo, M.D. Perkins, C.J. Roberts, Journal of Pharmaceutical Sciences 99 (2010) 4830–4848.
[80] H. Maity, C. O'Dell, A. Srivastava, J. Goldstein, Current Pharmaceutical Biotechnology 10 (2009) 761–766.
[81] M.J. Johnston, G. Frahm, X. Li, Y. Durocher, M.A. Hefford, Pharmaceutical Research 28 (2011) 1661–1667.
[82] T. Palm, R. Esfandiary, R. Gandhi, Pharmaceutical Development and Technology 16 (2011) 441–448.
[83] B. Plesner, P. Westh, A.D. Nielsen, International Journal of Pharmaceutics 406 (2011) 62–68.
[84] B. Plesner, P. Westh, A.D. Nielsen, European Journal of Pharmaceutics and Biopharmaceutics official : Journal of Arbeitsgemeinschaft fur Pharmazeutische Verfahrenstechnik e.V 78 (2011) 222–228.
[85] P. Sundaramurthi, R. Suryanarayanan, Pharmaceutical Research 27 (2010) 2384–2393.
[86] M.J. Pikal, D. Rigsbee, M.J. Akers, Journal of Pharmaceutical Sciences 98 (2009) 1387–1399.
[87] B. Wang, M.T. Cicerone, Y. Aso, M.J. Pikal, Journal of Pharmaceutical Sciences 99 (2010) 683–700.
[88] W. Cheng, S.B. Joshi, F. He, D.N. Brems, B. He, B.A. Kerwin, D.B. Volkin, C.R. Middaugh, Journal of Pharmaceutical Sciences 101 (2012) 1701–1720.
[89] S.V. Thakkar, S.B. Joshi, M.E. Jones, H.A. Sathish, S.M. Bishop, D.B. Volkin, C.R. Middaugh, Journal of Pharmaceutical Sciences (2012). 3062–3077.
[90] J.M. Sanchez-Ruiz, Biophysical Chemistry 126 (2007) 43–49.
[91] J.F. Brandts, L.N. Lin, Biochemistry 29 (1990) 6927–6940.
[92] D.E. Davidson, B.C. Hill, Biochimica et Biophysica Acta 1794 (2009) 275–281.
[93] J.M. Sayer, J.M. Louis, Proteins 75 (2009) 556–568.
[94] C.M. Dobson, Protein and Peptide Letters 13 (2006) 219–227.
[95] B. Morel, L. Varela, F. Conejero-Lara, The Journal of Physical Chemistry. B 114 (2010) 4010–4019.
[96] K. Sasahara, H. Yagi, H. Naiki, Y. Goto, Journal of Molecular Biology 372 (2007) 981–991.
[97] K. Sasahara, H. Yagi, H. Naiki, Y. Goto, Biochemistry 46 (2007) 3286–3293.
[98] N.C. Garbett, C.S. Mekmaysy, C.W. Helm, A.B. Jenson, J.B. Chaires, Experimental and Molecular Pathology 86 (2009) 186–191.
[99] N.C. Garbett, J.J. Miller, A.B. Jenson, J.B. Chaires, Biophysical Journal 94 (2008) 1377–1383.
[100] A.A. Chagovetz, R.L. Jensen, L. Recht, M. Glantz, A.M. Chagovetz, Journal of Neuro-oncology 105 (2011) 499–506.
[101] S. Todinova, S. Krumova, L. Gartcheva, C. Robeerst, S.G. Taneva, Analytical Chemistry 83 (2011) 7992–7998.
[102] J. Monaselisdze, T. Lezhava, G. Nemsadze, L. Kikalishvili, M. Ramishvili, Georgian Medical News (2011) 88–91.